

# Masking preprocessing in transfer learning for damage building detection

Hapnes Toba<sup>1</sup>, Hendra Bunyamin<sup>2</sup>, Juan Elisha Widyaya<sup>1</sup>, Christian Wibisono<sup>1</sup>,  
Lucky Surya Haryadi<sup>1</sup>

<sup>1</sup>Master Program in Computer Science, Faculty of Information Technology, Maranatha Christian University, Bandung, Indonesia

<sup>2</sup>Bachelor Program in Informatics Engineering, Faculty of Information Technology, Maranatha Christian University, Bandung, Indonesia

## Article Info

### Article history:

Received Jan 12, 2022

Revised Oct 10, 2022

Accepted Nov 9, 2022

### Keywords:

Classification

Convolutional neural network

Damage building detection

Image segmentation

Transfer learning

## ABSTRACT

The sudden climate change occurring in different places in the world has made disasters more unpredictable than before. In addition, responses are often late due to manual processes that have to be performed by experts. Consequently, major advances in computer vision (CV) have prompted researchers to develop smart models to help these experts. We need a strong image representation model, but at the same time, we also need to prepare for a deep learning environment at a low cost. This research attempts to develop transfer learning models using low-cost masking pre-processing in the experimental building damage (xBD) dataset, a large-scale dataset for advancing building damage assessment. The dataset includes eight types of disasters located in fifteen different countries and spans thousands of square kilometers of satellite images. The models are based on U-Net, i.e., AlexNet, visual geometry group (VGG)-16, and ResNet-34. Our experiments show that ResNet-34 is the best with an F1 score of 71.93%, and an intersection over union (IoU) of 66.72%. The models are built on a resolution of 1,024 pixels and use only first-tier images compared to the state-of-the-art baseline. For future orientations, we believe that the approach we propose could be beneficial to improve the efficiency of deep learning training.

*This is an open access article under the [CC BY-SA](#) license.*



## Corresponding Author:

Hapnes Toba

Master Program in Computer Science, Faculty of Information Technology,

Maranatha Christian University

Jl. Suria Sumantri No. 65, Bandung 40164, West Java, Indonesia

Email: hapnestoba@it.maranatha.edu

## 1. INTRODUCTION

A considerable amount of unprecedented weather changes around the world have made disasters more unpredictable and more severe than before [1]. On the other hand, the advance in machine learning (ML) and computer vision (CV) has brought computer science algorithms the capability of building intelligent and independent solutions for disaster prevention all around the world. Additionally, the increasing availability of satellite images from the United States and European scientific agencies, such as the United States Geological Survey (USGS), National Oceanic and Atmospheric Administration (NOAA), and European Space Agency (ESA) has further cultivated more and more research on ML and CV with the help of domain experts, such as humanitarian assistance and disaster recovery (HADR) and remote sensing experts [2]–[4]. Training accurate and robust CV models needs large-scale and a variety of datasets; moreover, all buildings have different designs from one another. The differences between designs depend on locations or countries where the buildings are located. It may seem a challenge for CV models to recognize all types of building from various places.

The experimental building damage (xBD) dataset [2] comprises satellite images utilized for detecting building shapes and assessing building damages. Furthermore, the dataset encompasses eight types of disasters located in fifteen different countries and covers thousands of square-kilometer satellite images. The dataset consists of pairs of images; specifically, the first and second images represent conditions of a region before and after a disaster respectively. Additionally, the dataset has been annotated in javascript object notation (JSON) form; therefore, there is no need for further annotation processes. This research attempts to build CV models which are capable of detecting and segmenting building shapes on satellite images before and after disasters occur.

One of the important issues in image processing is the complexity during the feature extraction process. In this sense, we need a powerful image representation model, but on the other hand, we also need to prepare for a low-cost deep learning environment. In this research, our main research question is thus, how to prepare a simple yet powerful image preprocessing for transfer learning.

The transfer learning approach has been chosen for the approach of this research because the technique has utilized best practices for state-of-the-art models [5]–[7]. Particularly, the trained models for detecting building shapes from given images employ convolutional neural networks (CNN) architectures such as AlexNet [8], visual geometry group (VGG) [9], and ResNet [10]. Furthermore, we postulate that by using a low complexity pre-processing algorithm, the entire transfer learning process will be more efficient.

## 2. METHOD

### 2.1. State-of-the-art techniques

Image segmentation refers to segmenting or partitioning an image into different areas, with each area commonly representing a class. Specifically, CV techniques can be employed on satellite images to extract a partition of the image as an object of a predefined class. Various techniques for satellite image segmentation consist of thresholding, clustering, region-based, and artificial neural networks (ANN). Among those techniques, ANN proves to be giving the best accuracy [11].

CNN is known as one of the deep learning techniques used for CV tasks. Specifically, CNN is developed from multilayer perceptron (MP) to process two-dimensional data such as images [7], [12], [13]. CNN technique has three layers which are divided into two main parts, feature learning, and classifier parts. The feature learning part consists of convolution layers and pooling layers. The classifier part comprises a fully connected layer. Arrangements of CNN shall construct various forms of CNN architectures such as AlexNet [8], VGG [9], and ResNet [10].

U-Net has the capability of processing large-size images and generating outputs whose sizes are the same as the ones of inputs. Another advantage of U-Net is the processing speed which is constant during the training phase. The U-Net training process adopts the CNN training method which replaces a pooling operation with the upsampling operation so the convolutional and pooling layers of the model can return the size of an input image [14]. The u-Net architecture resembles a letter U which is divided into contracting and expansive parts. A contracting part tackles the feature extraction process while an expansive part involves transferring features and reconstructing images to the original input size.

Previous satellite image datasets before xBD only cover one type of natural disaster with various label criteria for damaged buildings [4], [15], [16]. Furthermore, datasets [17], and [18] provide locations of disaster occurrences; however, these datasets do not include damaged building structure images. There are also datasets with multi-view imagery such as change detection and land classification [19]–[21] where several visits to one site and a time series of satellite images are provided. Prominent satellite image segmentation techniques are applied to road segmentation; specifically, the techniques are unsupervised [22], [23]. However, there are limited amounts of literature that discuss road segmentation and identification with obstructions. Other segmentation approaches to detect damaged buildings propose a ML model trained on non-building shapes. [24]. Ronneberger *et al.* [14] develop a U-Net architecture whose model is specifically designed to segment objects in medical images with a limited size of training data. They employ both the Glioblastoma-astrocytoma U373 cells on a polyacrylamide substrate (PhC-U373) and the Henrietta Lacks cells on a flat glass recorded by differential interference contrast microscopy (DIC-HeLa) datasets to measure the model's intersection over union (IoU) value. The IoU values for PhC-U373 and DIC-HeLa datasets are 0.9203 and 0.7756 respectively. Gupta *et al.* [2] establish a baseline model for the xBD dataset. Particularly, they utilize SpaceNet, a variant of U-Net architecture as shown in Figure 1. The IoU values of their model for ground and building are 0.97 and 0.66 respectively. Kurama *et al.* [11] use U-Net architecture trained on 2,000 images of the defence science and technology laboratory (DSTL) dataset and achieve 98% accuracy.

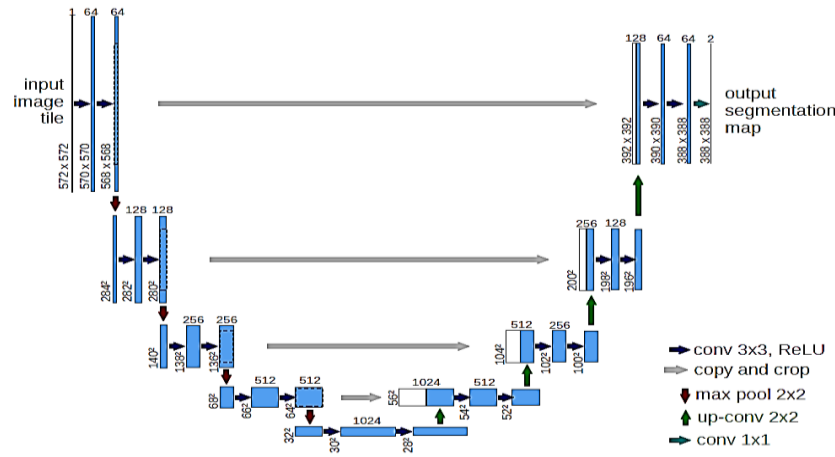


Figure 1. U-Net architecture [10]

## 2.2. Contributions

This research contributes to CV recent literature in the following aspects:

- We experimented with a lightweight masking preprocessing procedure for the disaster images in the xBD dataset which gives low complexity yet powerful feature extraction in the U-Net architectures.
- We compare several variants of CNN U-Net architectures utilized for detecting building shapes before and after disasters from the xBD dataset. The CNN segmentation techniques analyzed in this research are AlexNet, VGG-16, and ResNet-34 as these techniques are the most widely used in the literature [5].

We believe that this research shall give some insights into the masking preprocessing procedure and its potential during transfer learning. As far as we know. Our research is the first which compares the original experiment in the xBD dataset in various U-Net architectures.

## 2.3. Experiments

### 2.3.1. Dataset

This research uses the xBD dataset which is one of the publicly available annotated satellite images with high resolution. The dataset has more than 850,000 polygons for 22,000 building images from six types of disasters worldwide, which encompass more than 45,000 square kilometers [2]. The dataset annotations are done by experts in their fields such as California air national guard (CAL FIRE) and federal emergency management agency (FEMA). Each satellite image has red green blue (RGB) values which form three squares of 1,024 pixels. In this research, the first tier of the dataset is used and divided by xView2 into two portions, train and validation set. The number of images in the train set and validation set is 5,598 and 1,866 respectively which consist of the types of disasters described in Table 1.

Table 1. Number of images for each disaster

Disaster	Number of images	
	Train	Validation
guatemalare-volcano	36	10
hurricane-orence	638	238
hurricane-harvey	638	190
hurricane-matthew	476	188
hurricane-michael	686	218
mexico-earthquake	242	68
midwest-flooding	558	172
palu-tsunami	226	82
santa-rosa-wildfire	452	154
socal-fire 1,646 546	1,646	546
Total	5,598	1,866

### 2.3.2. Image preprocessing

The xBD dataset annotations are saved into JSON format and one of the annotations is building information coordinates on an image. Furthermore, this coordinate information is preprocessed into creating

a masking image [25]. The masking image consists of two classes, which are ground and building. A zero-value pixel in a masking image refers to a ground; on the other hand, a one-value pixel indicates a building. Figures 2 and 3 show an image before and after the masking process is applied. Furthermore, the masking image is used as a label or target during the training of a CV model.



Figure 2. An image before masking



Figure 3. An image after masking is applied

### 2.3.3. Model training

A model ( $f$ ) is trained on satellite images to detect buildings at pixel levels shows in Algorithm 1, that is:

#### Algorithm 1 Preprocessing images algorithm

```

1: procedure Preprocessing (images, json_file)
2: read the json_file containing building coordinates
3: for each image in images do
4:   for each pixel ( $i, j$ ) in the image do
5:     if ( $i, j$ ) is part of a building then #utilize the JSON file
6:       ( $i, j$ ) = 1
7:     else
8:       ( $i, j$ ) = 0

```

For every pixel in an image,  $p_{ij}$  with  $(i, j)$  as the coordinate of the pixel. This training method is a well-known technique known as image segmentation in CV literature [26]. We opt to choose the transfer learning approach as this approach gives the best performance results which are elaborated by Raffel *et al.* [27]. The convolutional base of CNN has been trained on the ImageNet dataset [5]; therefore, the xBD dataset is normalized by the statistics of ImageNet to have the same range of input distribution [28]. An illustration of the transfer learning approach is Figure 4.

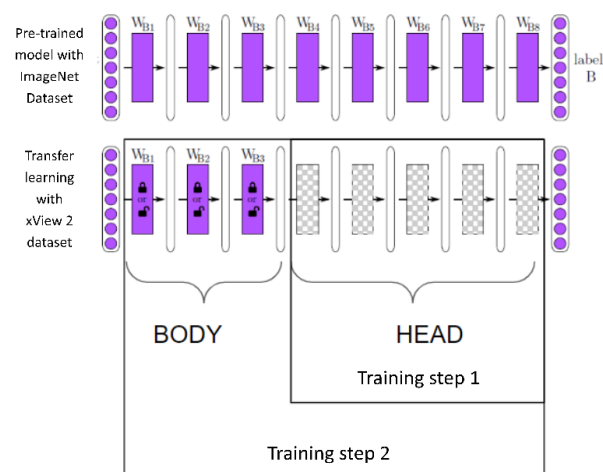


Figure 4. Transfer learning approach illustration

The transfer learning approach utilizes a convolutional base learner which has learned a lot of features from a dataset for a specific task. Next, this knowledge will be used to perform the task on a different dataset without initializing weights randomly. If the dataset is quite large, the weights of the model can be updated wholly; this training process is commonly called fine-tuning. Similarly, our model undergoes a two-stage training process. Firstly, only the head of the model is trained on the dataset. Next, the model is trained for updating the weights of all layers [29].

The deep learning library which was used during the training is fast.ai which is run on n1-highmem-4 and graphics processing unit (GPU) NVidia tesla T4 of google cloud platform for 4 days the learning rate is 0.0003 obtained from the cyclical learning rate finder algorithm [30]. During training, data augmentation techniques such as flipping images horizontally, rotating images, magnifying images, adjusting brightness, contrasting images, and wrapping images are also used. In addition, the performance parameters for this task are precision, recall, and F1, given in (1)-(3), with true positive (TP), false positive (FP), and false negative (FN) carefully assessed.

$$Precision = \frac{TP}{TP + FP} \quad (1)$$

$$Recall = \frac{TP}{TP + FN} \quad (2)$$

$$F1 = \frac{2 \times Precision \times Recall}{Precision + Recall} \quad (3)$$

Additionally, IoU metric in (4), the metric used in Gupta *et al.* [2], is also utilized to evaluate our model.

$$IoU = \frac{Area\ of\ Overlap}{Area\ of\ Union} \quad (4)$$

### 3. RESULTS AND DISCUSSION

Three CNN-based architectures, *i.e.*: AlexNet, VGG-16, and ResNet-34, are trained on 512 by 512-pixel images with 10 epochs. Our best-performing models are chosen based on the F1 score because of the imbalance between ground and building image instances in our dataset. The comparison of the three models when only the heads are trained is displayed in Table 2.

The best model among the three models, that is ResNet-34 is trained on 512 and 1,024 pixels on the head only with the number of epochs of 40 and a learning rate of 0.0003. Next, all layers are fine-tuned with a learning rate ranging from 0.000001 to 0.0001. Results of the training process are Tables 3 and 4. Both tables display that the models give better F1 scores and IoU results than the ones in Table 2.

Table 2. Comparison of the three models at the tenth epoch

Model	Accuracy	Precision	Recall	F1 Score
AlexNet	0.950	0.640	0.271	0.357
VGG-16	0.958	0.696	0.391	0.474
ResNet-34	0.966	0.700	0.674	0.683

Table 3. Training ResNet-34 model at 512 pixels resolution

Train	Accuracy	Precision	Recall	F1 Score	Mean IoU Building
Head	0.974	0.803	0.708	0.751	0.592
Fine-tuning	0.975	0.804	0.720	0.758	0.609

Table 4. Training ResNet-34 model at 1,024 pixels resolution

Train	Accuracy	Precision	Recall	F1 Score	Mean IoU Building
Head	0.978	0.789	0.681	0.719	0.667
Fine-tuning	0.978	0.791	0.676	0.717	0.669

Figure 5 presents a sample of our ground truth pixel values, while Figure 6 presents the predictions. The performances of the trained model on the validation set are measured by IoU [14], specifically the IoU building. Table 5 (512 pixels) and Table 6 (1,024 pixels) depict the segmentation results and IoU values of the

validation set from ten disasters. Image segmentation of hurricane-matthew gives the least value while the one of guatemala-volcano surprisingly displays a good result considering the size of its dataset which is the least.

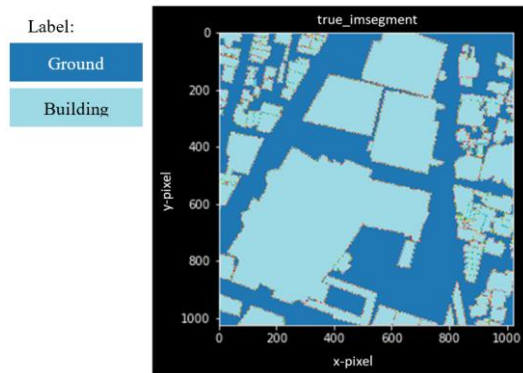


Figure 5. The ground truth pixel values of one sample in the validation set. The image size is 1,024×1,024 pixels (in the x and y-axis directions)

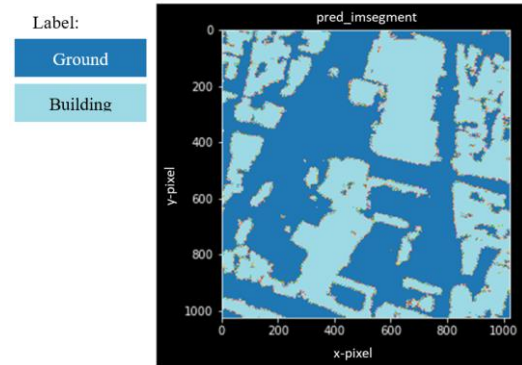


Figure 6. The predicted pixel values of the sample. The image size is 1,024×1,024 pixels (in the x and y-axis directions)

Table 5. IoU of disasters at 512 pixels resolution

Disaster	IoU segmentation at 512 pixels per disaster			
	Training Head		Fine Tuning	
	IoU ground	IoU building	IoU ground	IoU building
guatemala-volcano	0.992716	0.516159	0.992850	0.528130
hurricane-florence	0.996835	0.651713	0.996637	0.666267
hurricane-harvey	0.976307	0.672333	0.975674	0.688640
hurricane-matthew	0.993617	0.276589	0.993091	0.314112
hurricane-michael	0.986097	0.675072	0.985711	0.689483
mexico-earthquake	0.905966	0.671344	0.902866	0.687535
midwest-	0.994258	0.640343	0.994310	0.656130
palu-tsunami	0.953890	0.700680	0.947037	0.729558
santa-rosa-wildfire	0.986534	0.623966	0.986657	0.638125
socal-fire	0.996651	0.532794	0.996702	0.541918

Table 6. IoU of disasters at 1,024 pixels resolution

Disaster	IoU segmentation at 512 pixels per disaster			
	Training Head		Fine Tuning	
	IoU ground	IoU building	IoU ground	IoU building
guatemala-volcano	0.995799	0.582504	0.995598	0.577696
hurricane-florence	0.997853	0.744014	0.997796	0.749505
hurricane-harvey	0.978948	0.734031	0.979413	0.731891
hurricane-matthew	0.994308	0.364812	0.994263	0.375385
hurricane-michael	0.988052	0.742830	0.987936	0.742655
mexico-earthquake	0.914349	0.705674	0.916219	0.700831
midwest-	0.996147	0.726253	0.996176	0.726788
palu-tsunami	0.957746	0.742502	0.958971	0.744839
santa-rosa-wildfire	0.989383	0.708836	0.989252	0.700055
socal-fire	0.997107	0.611816	0.997081	0.614974

#### 4. CONCLUSION

This research delves into satellite image segmentation using a U-Net architecture with convolutional bases such as AlexNet, VGG-16, and ResNet-34. The final model is ResNet-34 with an accuracy of 0.978409, precision of 0.789098, recall of 0.681466, and F1-score of 0.719300 when the head of the model is trained. The mean of the IoU is 0.667237, and this number is similar to the IoU of our baseline as reported in the initial xBD dataset exploration. However, our research utilizes a smaller dataset, which is only the first tier compared to the baseline. Moreover, our architecture is simpler than the one of the baseline, that is ResNet-34. We also trained the model in 4 days compared to the baseline which is in 7 days. These advantages can be achieved because of the transfer learning approach. For future directions, we believe that our proposed method can be beneficial to improve the training efficiency in deep learning. It is strongly

recommended to cooperate with satellite image experts to obtain in-depth interpretation and information. Furthermore, a greater number of images should also give better performances at detecting buildings from satellite images. Consequently, models can be improved to detect levels of damage to buildings after successful segmentation.

## ACKNOWLEDGEMENTS

The research presented in this paper was partially supported by the Research Institute and Community Service (LPPM) at Maranatha Christian University, Indonesia.

## REFERENCES




- [1] M. K. Van Aalst, "The impacts of climate change on the risk of natural disasters," *Disasters*, vol. 30, no. 1, pp. 5–18, Mar. 2006, doi: 10.1111/j.1467-9523.2006.00303.x.
- [2] R. Gupta *et al.*, "xBD: A Dataset for Assessing Building Damage from Satellite Imagery," Nov. 2019, [Online]. Available: <http://arxiv.org/abs/1911.09296>.
- [3] S. Dhingra and D. Kumar, "A review of remotely sensed satellite image classification," *International Journal of Electrical and Computer Engineering (IJECE)*, vol. 9, no. 3, p. 1720, Jun. 2019, doi: 10.11591/ijece.v9i3.pp1720-1731.
- [4] R. Foulser-Piggott, R. Spence, R. Eguchi, and A. King, "Using remote sensing for building damage assessment: GEOCAN study and validation for 2011 Christchurch earthquake," *Earthquake Spectra*, vol. 32, no. 1, pp. 611–631, Feb. 2016, doi: 10.1193/051214EQS067M.
- [5] F. Zhuang *et al.*, "A comprehensive survey on transfer learning," *Proceedings of the IEEE*, vol. 109, no. 1, pp. 43–76, Jan. 2021, doi: 10.1109/JPROC.2020.3004555.
- [6] M. S. AL-Huseiny and A. S. Sajit, "Transfer learning with GoogLeNet for detection of lung cancer," *Indonesian Journal of Electrical Engineering and Computer Science*, vol. 22, no. 2, p. 1078, May 2021, doi: 10.11591/ijeecs.v22.i2.pp1078-1086.
- [7] M. Moe Htay, "Feature extraction and classification methods of facial expression: a survey," *Computer Science and Information Technologies*, vol. 2, no. 1, pp. 26–32, Mar. 2021, doi: 10.11591/csit.v2i1.p26-32.
- [8] A. Krizhevsky, I. Sutskever, and G. E. Hinton, "ImageNet classification with deep convolutional neural networks," *Communications of the ACM*, vol. 60, no. 6, pp. 84–90, 2017, doi: 10.1145/3065386.
- [9] K. Simonyan and A. Zisserman, "Very deep convolutional networks for large-scale image recognition," vol. 1, Sep. 2014, [Online]. Available: <http://arxiv.org/abs/1409.1556>.
- [10] H. Imaduddin, F. Yusufida Ala, A. Fatmawati, and B. A. Hermansyah, "Comparison of transfer learning method for COVID-19 detection using convolution neural network," *Bulletin of Electrical Engineering and Informatics*, vol. 11, no. 2, pp. 1091–1099, Apr. 2022, doi: 10.11591/eei.v11i2.3525.
- [11] V. Kurama, S. Alla, and S. Tumula, "Detection of natural features and objects in satellite images by semantic segmentation using neural networks," *Artificial Intelligence Techniques for Satellite Image Analysis*, pp. 161–188, 2020, doi: 10.1007/978-3-030-24178-0\_8.
- [12] J. Wu, "Introduction to convolutional neural networks," *National Key Lab for Novel Software Technology*, vol. 5, no. 23, p. 495, 2017.
- [13] Y. H. Liu, "Feature extraction and image recognition with convolutional neural networks," *Journal of Physics: Conference Series*, vol. 1087, p. 62032, Sep. 2018, doi: 10.1088/1742-6596/1087/6/062032.
- [14] O. Ronneberger, P. Fischer, and T. Brox, "U-Net: Convolutional Networks for Biomedical Image Segmentation," in *International Conference on Medical image computing and computer-assisted intervention*, 2015, pp. 234–241.
- [15] W. Shi, M. Zhang, R. Zhang, S. Chen, and Z. Zhan, "Change detection based on artificial intelligence: state-of-the-Art and challenges," *Remote Sensing*, vol. 12, no. 10, p. 1688, May 2020, doi: 10.3390/rs12101688.
- [16] S. A. Chen, A. Escay, C. Haberland, T. Schneider, V. Staneva, and Y. Choe, "Benchmark dataset for automatic damaged building detection from post-hurricane remotely sensed imagery," Dec. 2018, [Online]. Available: <http://arxiv.org/abs/1812.05581>.
- [17] L. Giglio, J. T. Randerson, and G. R. van der Werf, "Analysis of daily, monthly, and annual burned area using the fourth-generation global fire emissions database (GFED4)," *Journal of Geophysical Research: Biogeosciences*, vol. 118, no. 1, pp. 317–328, Mar. 2013, doi: 10.1002/jgrg.20042.
- [18] I. Demir *et al.*, "DeepGlobe 2018: a challenge to parse the earth through satellite images," in *2018 IEEE/CVF Conference on Computer Vision and Pattern Recognition Workshops (CVPRW)*, Jun. 2018, pp. 172–17209, doi: 10.1109/CVPRW.2018.00031.
- [19] J. Ding *et al.*, "Object detection in aerial images: A large-scale benchmark and challenges," *IEEE Transactions on Pattern Analysis and Machine Intelligence*, p. 1, 2021, doi: 10.1109/TPAMI.2021.3117983.
- [20] D. Ienco, R. Gaetano, C. Dupaquier, and P. Maurel, "Land cover classification via multitemporal spatial data by deep recurrent neural networks," *IEEE Geoscience and Remote Sensing Letters*, vol. 14, no. 10, pp. 1685–1689, Oct. 2017, doi: 10.1109/LGRS.2017.2728698.
- [21] D. Peng, Y. Zhang, and H. Guan, "End-to-End change detection for High desolution satellite images using improved UNet++," *Remote Sensing*, vol. 11, no. 11, p. 1382, Jun. 2019, doi: 10.3390/rs11111382.
- [22] Z. Zhang, Q. Liu, and Y. Wang, "Road extraction by deep residual U-Net," *IEEE Geoscience and Remote Sensing Letters*, vol. 15, no. 5, pp. 749–753, May 2018, doi: 10.1109/LGRS.2018.2802944.
- [23] A. Buslaev, V. I. Iglovikov, E. Khvedchenya, A. Parinov, M. Druzhinin, and A. A. Kalinin, "Albumentations: Fast and flexible image augmentations," *Information (Switzerland)*, vol. 11, no. 2, 2020, doi: 10.3390/info11020125.
- [24] Z.-Q. Zhao, P. Zheng, S.-T. Xu, and X. Wu, "Object detection with deep learning: a review," *IEEE Transactions on Neural Networks and Learning Systems*, vol. 30, no. 11, pp. 3212–3232, Nov. 2019, doi: 10.1109/TNNLS.2018.2876865.
- [25] H. Bunyamin, "Creating mask images from shapely polygons," *Creating Mask Images from Shapely Polygons*. 2022, Accessed: Jun. 28, 2022. [Online]. Available: [https://hbunyamin.github.io/computer-vision/Creating\\_Masks/](https://hbunyamin.github.io/computer-vision/Creating_Masks/).
- [26] J. Guo *et al.*, "GluonCV and gluon NLP: Deep learning in computer vision and natural language processing," *Journal of Machine Learning Research*, vol. 21, no. 23, pp. 1–7, 2020.
- [27] C. Raffel *et al.*, "Exploring the limits of transfer learning with a unified text-to-text transformer," *Journal of Machine Learning Research*, vol. 21, no. 140, pp. 1–67, 2020.






- [28] P. Mettes, D. C. Koelma, and C. G. M. Snoek, "Shuffled imageNet banks for video event detection and search," *ACM Transactions on Multimedia Computing, Communications, and Applications*, vol. 16, no. 2, pp. 1–21, May 2020, doi: 10.1145/3377875.
- [29] J. Howard and S. Gugger, "Fastai: A layered api for deep learning," *Information (Switzerland)*, vol. 11, no. 2, 2020, doi: 10.3390/info11020108.
- [30] L. N. Smith, "No more pesky learning rate guessing games," *CoRR Abs150601186*, vol. 5, p. 363, 2015.

## BIOGRAPHIES OF AUTHOR






**Hapnes Toba**    graduated in 2002 with a Master of Science from the Delft University of Technology in the Netherlands and completed his doctoral degree in computer science at Universitas Indonesia in 2015. He is an associate professor in the area of artificial intelligence and is interested in information retrieval, natural language processing, and computer vision. He has been a faculty member in the Faculty of Information Technology at Maranatha Christian University since 2003. He is also an active board member of the Indonesian Computational Language Association (INACL) and the vice-chair of the Information and Communication Technology Forum (FTIK) of the Association of Christian Universities and Colleges in Indonesia (BK-PTKI). He can be contacted by email at: hapnestoba@it.maranatha.edu.






**Hendra Bunyamin**    is an assistant professor at the Faculty of Information Technology at Maranatha Christian University, Bandung, Indonesia. He graduated from the Mathematics Department at Bandung Institute of Technology in 1999 and pursue his master's degree from the Software Engineering, Informatics Department at the same university in 2005. He is very passionate about teaching mathematics and programming. His research focuses on the application techniques of automatic learning algorithms. He can be contacted by email at: hendra.bunyamin@it.maranatha.edu.






**Juan Elisha Widyaya**    graduated in 2012 with a Bachelor of Engineering degree and 2021 with a Master of Computer Science degree, both from Maranatha Christian University. He has an interest in pattern recognition, deep learning, computer vision, and time series analysis. Since 2012 he has been working at PT. Yamaha Indonesia Motor Manufacturing as an Area Service Development. He can be contacted at email: 1979006@maranatha.ac.id.



**Christian Wibisono**    graduated in 2021 with a Master of Computer Science from Maranatha Christian University. He is currently working at a manufacturing company as an IT Assistant Manager. He is a passionate software engineer specializing in React, GraphQL, Next JS, PL/SQL, and SQL. He is passionately studying machine learning and deep learning technology to expand his knowledge in this field, so soon he can implement this knowledge to support the needs of the business. He can be contacted at email: 1979002@maranatha.ac.id.



**Lucky Surya Haryadi**    graduated in 2021 with a Master of Computer Science from Maranatha Christian University. Lucky's research is focused on computer vision, social networks, and social media analytics. He decided to pursue his master's degree in computer science to improve small businesses with technological advancement. He is the founder of Mierakigai, a company that works in Social Media Advertising and Social Media Analytics. He can be contacted at email: suryaharyadi@gmail.com and 1979001@maranatha.ac.id.